PHILOSOPHICAL TRANSACTIONS OF THE ROYAL SOCIETY A MATHEMATICAL, PHYSICAL & ENGINEERING SCIENCES

Dynamics of Double Convection

D. R. Moore and N. O. Weiss

Phil. Trans. R. Soc. Lond. A 1990 **332**, 121-134
doi: 10.1098/rsta.1990.0104

Dynamics of double convection

By D. R. Moore[1] and N. O. Weiss[2]

[1] *Department of Mathematics, Imperial College of Science, Technology and Medicine, London SW7 2BZ, U.K.*

[2] *Department of Applied Mathematics and Theoretical Physics, University of Cambridge, Cambridge CB3 9EW, U.K.*

Double-diffusive convection provides examples of the competition between stabilizing and destabilizing mechanisms in fluid mechanics, leading to a rich variety of complicated nonlinear behaviour. Weakly nonlinear convection can be described analytically and fully nonlinear solutions have been obtained in a series of numerical experiments on two-dimensional thermosolutal convection and magnetoconvection. These provide examples of various bifurcation structures including interactions between standing waves, travelling waves and steady solutions, transitions to temporal chaos, loss of spatial symmetry and the development of spatiotemporal chaos. The behaviour found in the numerical experiments can be related to low-order systems derived as normal form equations for the appropriate degenerate bifurcations.

1. Introduction

The competition between stabilizing and destabilizing mechanisms in a dissipative system can lead to a rich variety of dynamical behaviour. Consider, for example, a fluid layer that is stabilized by a bottom-heavy solute gradient and then heated gently from below. If a blob of fluid is displaced it will oscillate about its equilibrium position and, since heat diffuses more rapidly than the solute, the oscillations can be maintained against viscous dissipation. Thus instability sets in at a Hopf bifurcation giving rise to a branch of oscillatory solutions. The oscillations may eventually become chaotic before giving way to steady overturning motion, so providing a nice example of temporal chaos in a continuous fluid system. Although earlier studies were devoted to complicated time-dependent behaviour with a relatively simple spatial structure current research is more concerned with changing spatial structures and the development of spatiotemporal chaos.

Thermosolutal convection can be realized in the laboratory in a layer with cold fresh water lying above hot salty water, or with a dissolved salt-sugar mixture (Huppert & Turner 1981). Binary fluids (water–ethanol or ^{3}He–^{4}He mixtures) are even more convenient for experiments (Walden *et al.* 1985; Ahlers & Rehberg 1986). Similar behaviour arises in a rotating system, if the viscosity is small, or in the presence of a magnetic field, if the electrical conductivity is large; here the Coriolis force or the Lorentz force exert stabilizing influences. Thermohaline convection occurs naturally in the oceans, e.g. beneath the Arctic ice sheet (Padman & Dillon 1987) while magnetic fields and convection interact in cool stars like the Sun (Hughes & Proctor 1988).

Phil. Trans. R. Soc. Lond. A (1990) **332**, 121–134 *Printed in Great Britain*

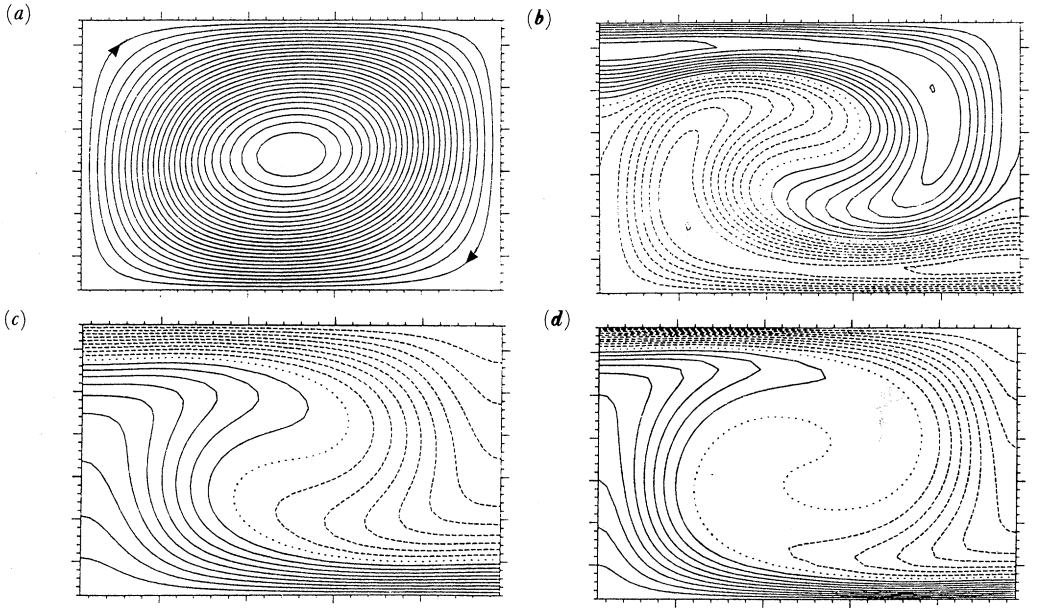

Figure 1. Steady thermosolutal convection with $R_S = 10^4$, $\sigma = 1$, $\tau = 10^{-\frac{1}{2}}$, $\lambda = 1.5$ and $R_T = 10\,800$. Contours of (*a*) ψ (streamlines), (*b*) ρ, (*c*) T (isotherms) and (*d*) S, after Moore *et al.* (1991). Positive (negative) values are indicated by full (broken) lines and the zero contour is indicated by a dotted line.

We shall focus our attention on an idealized model of thermosolutal convection. In the absence of motion there is a static (trivial) solution that corresponds to a uniformly stratified layer where the stabilizing gradient in solute concentration and the destabilizing temperature gradient are measured by a solutal Rayleigh number R_S and a thermal Rayleigh number R_T respectively, while the density gradient is proportional to $(R_T - R_S)$. We are interested in the régime where $R_S \gg 1$ and the ratio τ of the solutal to the thermal diffusivity is small, while the Prandtl number σ (the ratio of the viscous to the thermal diffusivity) remains of order unity. Then the layer is neutrally stratified if $R_T = R_S$ but double-diffusive effects allow oscillatory convection to set in when $R_T \approx [\sigma/(\sigma+1)]R_S < R_S$ (Knobloch *et al.* 1986*b*). The dynamically interesting régime occurs when $|R_T - R_S| \ll R_S$. Then the density ρ is almost constant for the static solution but any motion produces different distributions of solute concentration S and temperature T, owing to their different diffusivities, and therefore leads to large density gradients and interesting behaviour. This situation is illustrated for a steady two-dimensional solution in figure 1. The streamlines in figure 1*a* correspond to clockwise motion. In a steady state the competition between advection and diffusion forces both S and T to be almost uniform at the centre of the roll with rising and falling plumes at the sides, as shown by the contours in figure 1*c* and *d*. The narrower solute plumes are embedded in the broader thermal plumes. Hence ρ has the more complicated structure shown in figure 1*d* and vorticity with different senses is generated on either side of each plume (Moore *et al.* 1990*b*). It is apparent that time-dependent motion can immediately produce a complicated density pattern and so lead to exotic behaviour. The most interesting feature of this problem is the interaction between the underlying physics,

shown by the spatial structure of the flow, and the mathematical constraints imposed by bifurcation theory.

We shall outline the time-dependent behaviour found in numerical investigations of two-dimensional convection, emphasizing symmetries of the solutions and bifurcations that lead to loss of spatial symmetry or complicated time-dependence. The rich bifurcation structure found in these numerical experiments may be analysed by relating it to low-order model systems which can be studied in more detail. In particular, we rely on normal form equations that describe behaviour in the neighbourhood of degenerate bifurcations (Guckenheimer & Holmes 1986). First of all we discuss behaviour near the initial Hopf bifurcation, where travelling waves compete with oscillatory (standing-wave) solutions, and then we follow these solution branches until they meet the steady-solution branch. Next, in §3, we illustrate the transition to temporal chaos in a confined system; then, in §4, we look at loss of spatial symmetry and provide an example of spatiotemporal chaos. In conclusion, we explain how this simple model serves as a paradigm for more complicated systems.

2. Travelling waves and standing waves

We consider a Boussinesq fluid occupying the region $\{0 \leqslant x \leqslant \lambda;\ 0 < z < 1\}$. with

$$T = \tfrac{1}{2} - z + \theta(x, z, t), \quad S = \tfrac{1}{2} - z + \Sigma(x, z, t), \tag{1}$$

referred to cartesian coordinates. Then θ and Σ, the fluctuations in temperature and solute concentration, and the stream function $\psi(x, z, t)$ satisfy the equations

$$\partial_t \nabla^2 \psi + \partial(\psi, \nabla^2 \psi) = \sigma[R_T \partial_x \theta - R_S \partial_x \Sigma + \nabla^4 \psi], \tag{2}$$

$$\partial_t \theta + \partial(\psi, \theta) = \partial_x \psi + \nabla^2 \theta, \tag{3}$$

$$\partial_t \Sigma + \partial(\psi, \Sigma) = \partial_x \psi + \tau \nabla^2 \Sigma, \tag{4}$$

subject to the idealized boundary conditions

$$\psi = \partial_z^2 \psi = \theta = \Sigma = 0 \quad \text{at} \quad z = 0, 1. \tag{5}$$

For this section we assume periodic lateral boundary conditions so that

$$\psi(0, z) = \psi(\lambda, z), \quad \theta(0, z) = \theta(\lambda, z), \quad \Sigma(0, z) = \Sigma(\lambda, z). \tag{6}$$

The system (2)–(6) is unaffected by translations (modulo λ) in the x-direction or by reflection in the plane $x = 0$; thus it has $\mathrm{O}(2) = \mathrm{SO}(2) \times \mathrm{Z}_2$ symmetry in x together with the up-down symmetry

$$m_z: \quad (x, z) \to (x, 1-z),\ (\psi, \theta, \Sigma) \to (-\psi, -\theta, -\Sigma). \tag{7}$$

The trivial solution has O(2) symmetry. This is broken at the Hopf bifurcation, which gives rise to a branch of left- or right-ward travelling wave (TW) solutions with SO(2) symmetry, and a branch of standing wave (SW) solutions with Z_2 symmetry (Ruelle 1973; Stewart 1988). It can be shown that SW solutions are always unstable in the neighbourhood of the Hopf bifurcation for thermosolutal convection (Bretherton & Spiegel 1983; Knobloch *et al.* 1986*a*). We shall restrict our attention to numerical results obtained for $\sigma = 1$, $\tau = 10^{-\frac{1}{2}}$ and $R_S = 10^4$; for this section we set

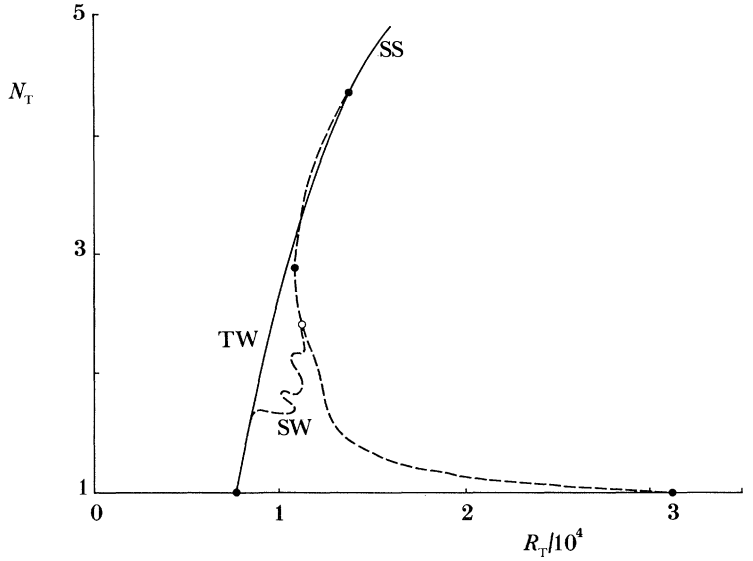

Figure 2. Bifurcation structure for modal system with O(2) symmetry, showing branches of standing wave (SW), travelling wave (TW) and steady (SS) solutions in the (R_T, N_T)-plane. Full (broken) lines indicate stable (unstable) solutions and filled (open) circles denote local (global) bifurcations. (The SS and TW branches were computed using eight horizontal modes but the SW branch is a composite, based mainly on solutions of the full equations.)

$\lambda = 3$. Then both branches bifurcate supercritically and TW are stable. Figure 2 shows a bifurcation diagram for this problem mainly computed using 8 horizontal modes (cf. Moore & Knobloch 1990). The ordinate is the thermal Nusselt number

$$N_T = 1 - \lambda^{-1} \int_0^\lambda \partial_z \theta \, dx, \tag{8}$$

evaluated at $z = 1$, and $(N_T - 1)$ provides a quadratic measure of convective efficiency. As R_T is increased there is a Hopf bifurcation at $R_T^{(o)} = 7725$ followed eventually by a pitchfork bifurcation at $R_T^{(e)} = 32283$, giving rise to a branch of unstable steady solutions (SS) which undergoes a saddle-node bifurcation at $R_T^{(min)} = 10670$ (Moore *et al.* 1991). Figure 1 illustrates the spatial structure of a solution on the upper part of the steady branch at $R_T = 10800$.

The TW and SW solutions are contrasted in figure 3 for $R_T = 10000$. The travelling wave progresses rightward without change of form and has a phase velocity $v = 18.87$; there is an equivalent solution with velocity $-v$. From figure 3*a–c* it is apparent that the TW solution possesses the symmetry

$$(x, z) \to (x + \tfrac{1}{2}\lambda, 1 - z), \quad (\psi, \theta, \Sigma) \to (-\psi, -\theta, -\Sigma) \tag{9}$$

in the comoving frame (Barten *et al.* 1989). The standing wave oscillates with a period $P = 0.288$ and possesses the symmetry

$$t_z: \quad (x, z, t) \to (x, 1 - z, t + \tfrac{1}{2}P), \quad (\psi, \theta, \Sigma) \to (-\psi, -\theta, -\Sigma) \tag{10}$$

so that advancing time by half a period is equivalent to reflection about $z = \frac{1}{2}$ (Weiss 1990*b*; Moore *et al.* 1991). At the Hopf bifurcation $P = \lambda/v$ and the period increases along the SW branch, becoming infinite when the branch terminates in a heteroclinic

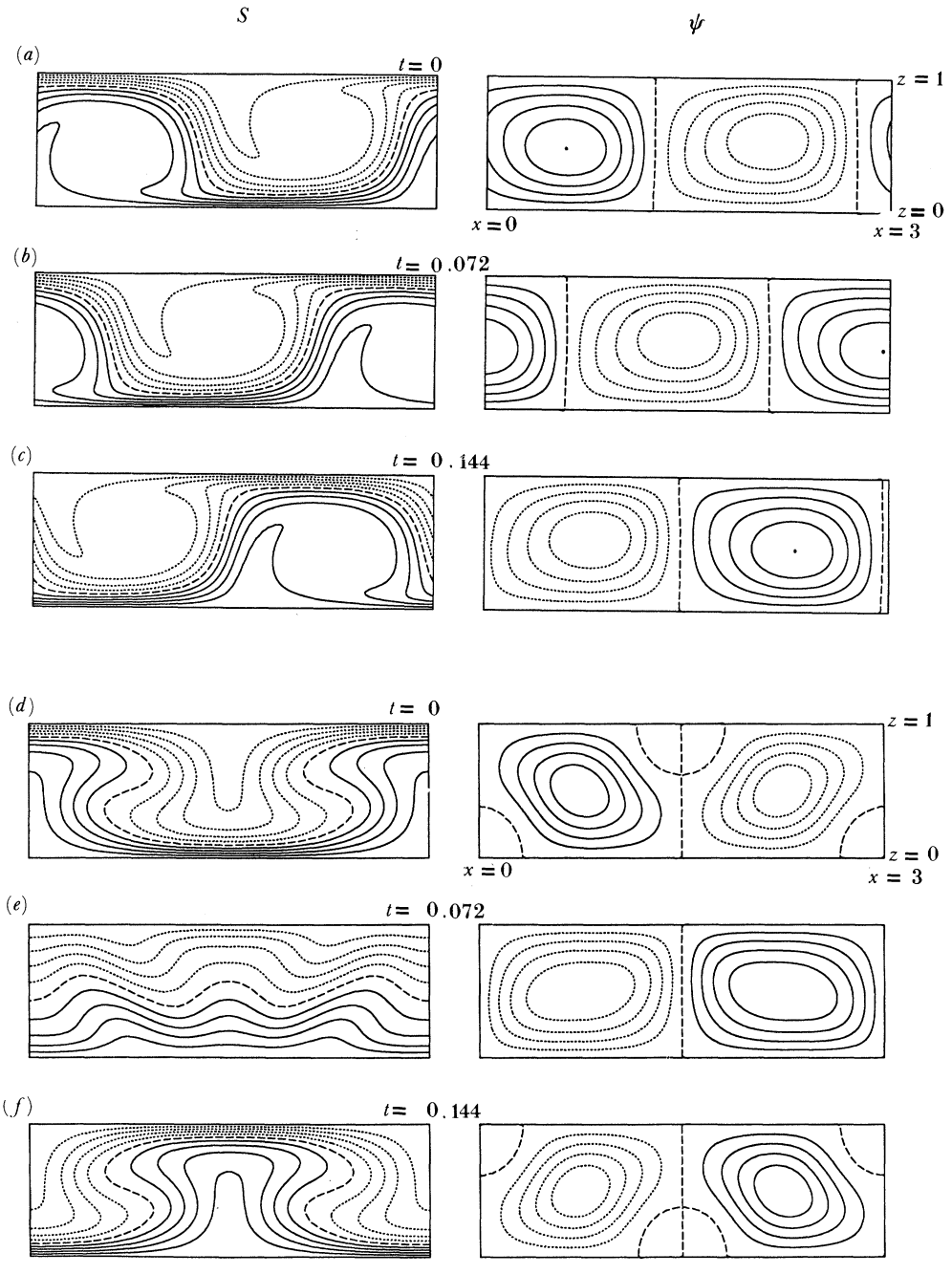

Figure 3. Standing wave and travelling wave solutions for the modal system with $R_T = R_S = 10^4$. (*a*), (*b*), (*c*) Contours of ψ and S for a leftward travelling wave at times $t = 0, 0.072, 0.144$. (*d*), (*e*), (*f*) The same but for a standing wave showing reversal of the flow.

bifurcation (see §3 below). The TW branch terminates in a supercritical pitchfork bifurcation from the SS branch at $R_T^{(TW)} = 14000$, where $v = 0$ (Deane *et al.* 1987; Knobloch & Moore 1990). Thus SW are always unstable and TW are the only stable solutions for $R_T^{(o)} < R_T < R_T^{(TW)}$ while SS are stable for $R_T > R_T^{(TW)}$. In other parameter ranges stability may be transferred from TW to a branch of modulated waves (MW) which terminates in a homoclinic bifurcation (Knobloch & Moore 1990); alternatively, the MW may provide a link to a subcritical SW branch which gains stability in a saddle-node bifurcation (Deane *et al.* 1987).

3. Chaos

Instead of the periodic lateral boundary conditions (6) we now impose reflection symmetry so that

$$\psi = \partial_x^2 \psi = \partial_x \theta = \partial_x \Sigma = 0 \quad \text{at} \quad x = 0, \lambda \tag{11}$$

and there is no flux of mass, heat or solute across the boundary. This restricts behaviour so that all solutions have Z_2 symmetry and TW are eliminated. For compatibility with the previous section we have to set $\lambda = 1.5$. The system now has the symmetry of a rectangle, represented by the dihedral group D_2; in particular, it possesses the point symmetry

$$i: \quad (x, z) \to (\lambda - x, 1 - z), \quad (\psi, \theta, \Sigma) \to (\psi, -\theta, -\Sigma) \tag{12}$$

(Weiss 1990*b*; Moore *et al.* 1991). The eigenfunctions of the linear problem, corresponding to rolls with a horizontal wavenumber π/λ, also possess this symmetry; hence the single-roll SW and SS solutions on branches emerging from $R_T^{(o)}$ and $R_T^{(e)}$ both possess point symmetry and the symmetry can only be broken at a bifurcation. In this section we describe the behaviour of solutions when the symmetry i is explicitly imposed, so that results from numerical experiments can be related to behaviour in low-order model systems. Breaking of spatial symmetry will be discussed in §4.

When $R_S = 0$ steady convection sets in at $R_T = R_0 \equiv \pi^4(1+\lambda^2)^3/\lambda^4$. As R_S is increased oscillatory instabilities appear for $R_S > R_S^{(c)} \equiv R_0 \tau^2(1+\sigma)/\sigma(1-\tau)$ provided $\tau < 1$. Nonlinear SW solutions were first computed by Veronis (1965, 1968). When $R_S = R_S^{(c)}$ there is a degenerate (Bogdanov) bifurcation with a double-zero eigenvalue at $R_T = R_T^{(c)} \equiv R_0 + R_S^{(c)}/\tau$. The relation between the oscillatory and steady branches can be established by considering weakly nonlinear behaviour when R_S, R_T are close to $R_S^{(c)}$ and $R_T^{(c)}$ (Knobloch & Proctor 1981; Coullet & Spiegel 1983). If the stream function $\psi = a(t) \sin(\pi x/\lambda) \sin \pi z + O(a^2)$ with $|a| \ll 1$ then its evolution is described by the Bogdanov–Takens normal form equation

$$\ddot{a} - (\mu - a^2)\dot{a} + (\nu - ka^2)a = 0, \tag{13}$$

where μ, ν are parameters and k is a positive constant (Arnol'd 1983; Guckenheimer & Holmes 1986). The codimension-two bifurcation occurs at the origin in the $\mu\nu$-plane; at $\nu = 0$ there is a line of pitchfork bifurcations and non-stable SS exist for $\nu > 0$. Hopf bifurcations lie on the half-line $\mu = 0$, $\nu > 0$ and the branch of oscillatory solutions terminates in a heteroclinic bifurcation, with an orbit of infinite period connecting a symmetric pair of saddle-points, when $\mu = \mu_c = (\nu/5k) + O(\nu^2)$. This pattern of behaviour is structurally stable: the bifurcation structure as R_T is increased for fixed R_S, corresponding to codimension-one behaviour obtained by

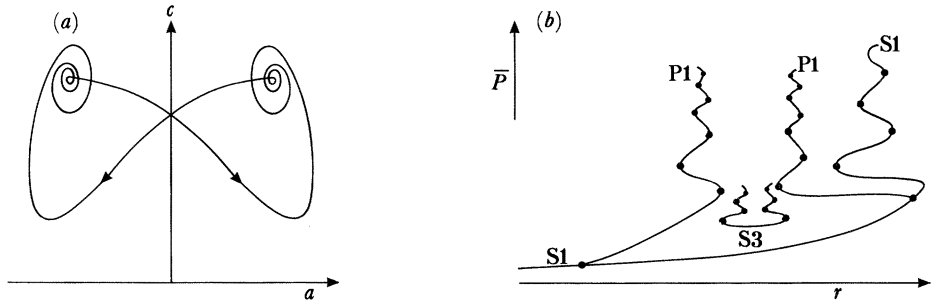

Figure 4. (*a*) Sketch of a heteroclinic trajectory connecting two saddle-foci projected onto the *ac*-plane. (*b*) Schematic bifurcation diagram showing the mean period $\bar{P}$ as a function of the bifurcation parameter μ for periodic solutions on the S1, P1, and S3 branches.

increasing μ with $\nu = \nu_0 - \mu$, say, in (13), is indicated in figure 2. Numerical experiments have confirmed the existence of a branch of SW solutions whose period P tends to infinity as the global bifurcation is approached (Huppert & Moore 1976; Knobloch *et al.* 1986*b*).

Weakly nonlinear behaviour in the neighbourhood of either the Hopf bifurcation at $R_{\mathrm{T}}^{(\mathrm{o})}$ or the pitchfork bifurcation at $R_{\mathrm{T}}^{(\mathrm{e})}$ is described by a fifth-order system of ordinary differential equations (Veronis 1965; Da Costa *et al.* 1981) which reduces to the third-order system

$$\ddot{a} - \mu\dot{a} + \nu a = ac - ka^3, \quad \dot{c} = \varpi(-c + a^3) \tag{14}$$

in the limit $\tau \to 0$, where $\varpi = 4\lambda^2(1+\lambda^2)$ and $k = \varpi/[\varpi + 2(1+\mu)]$ (Knobloch *et al.* 1990). The system (14) is equivalent to the well-known Lorenz equations (Sparrow 1982) in a slightly unfamiliar régime. If we again consider the double-zero bifurcation but restrict our attention to narrow rolls ($\lambda \ll 1$) and let $\varpi \downarrow 0$ then behaviour near the global bifurcation is governed by a simpler third-order system:

$$\ddot{a} - \mu\dot{a} + \nu a = ac, \quad \dot{c} = -c + a^2 \tag{15}$$

(Proctor & Weiss 1990). For $0.15 < \mu < 1$ the heteroclinic orbit now forms a connection between a symmetric pair of saddle-foci with eigenvalues $r, -p \pm iq (p, r > 0)$, as sketched in figure 4*a*. Moreover, the ratio $\delta \equiv p/r$ satisfies the condition $\frac{1}{2} < \delta < 1$ which guarantees the existence of stable chaos near the heteroclinic bifurcation (Shil'nikov 1965; Wiggins 1988).

As μ approaches μ_{c} the period P becomes very large and a plot of P against μ shows a series of wiggles as the orbit describes more turns around the saddle-focus as shown schematically in figure 4*b*. (Similar wiggles are visible in the actual bifurcation diagram of figure 3.) Solutions on this branch (denoted by S1) are still periodic and retain the symmetry t_z. Further bifurcations lead to chaos within bubbles on alternate wiggles. Initially there is a sequence of bifurcations from the symmetric S1 oscillations to asymmetric P1 oscillations, in which the symmetry t_z is broken, followed by a cascade of period-doubling bifurcations leading to chaos interspersed with periodic windows and then back through an inverse cascade to P1 and S1 solutions at the end of the wiggle, as indicated in figure 4*b* (cf. Glendinning & Sparrow 1984; Gaspard & Kapral 1984). The order in which these bifurcations occur

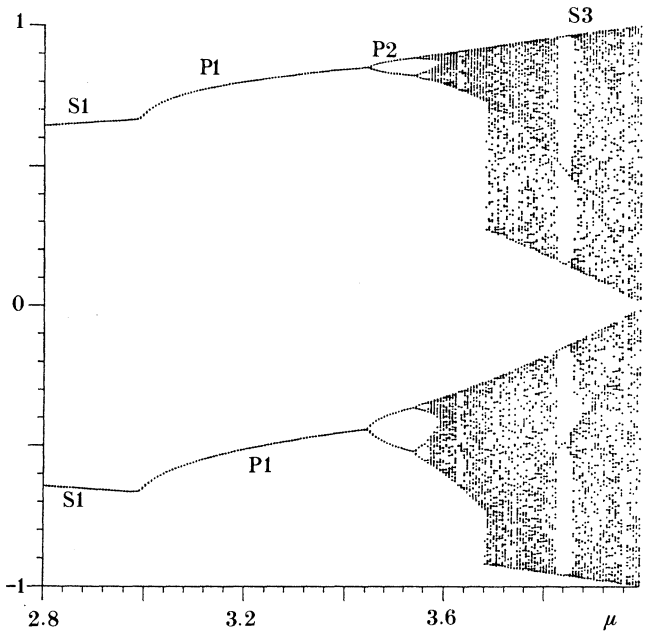

Figure 5. Attracting set for the map (16) showing iterates of x as a function of μ after transients have died away. Note the appearance of P1, P2, ..., solutions at successive bifurcations and the S3 periodic window. (After Proctor & Weiss 1990.)

follows that familiar from quadratic maps and is best represented by the modified logistic map

$$x \to -\mu x(1-|x|) \ (1 \geqslant \mu \geqslant 4) \tag{16}$$

(Proctor & Weiss 1990). Figure 5 shows the attracting set for this map in the interval $2.8 \geqslant \mu \geqslant 4$: note the transition from S1 solutions with the symmetry $x \to -x$ to asymmetric P1 solutions at $\mu = 3$, followed by period-doubling and chaos at $\mu = 3.57$ (May 1976). There is a transition from symmetric to asymmetric chaos at $\mu = 3.68$ and several periodic windows can be identified. Of these the most significant correspond to symmetric period 5 (S5) and period 3 (S3) solutions at $\mu = 3.74$ and $\mu = 3.83$ (Metropolis *et al.* 1973). The appearance of an S3 solution guarantees the presence of chaos and of all other periodicities, both for the map and for the ordinary differential equations. As ν increases the bubble structure grows more complicated. Figure 4*b* indicates how other solutions develop subsidiary homoclinicities. The P1 branches develop wiggles as the period increases. Similarly, the normalized period $\bar{P} = \frac{1}{3}P$ of the S3 orbits, which appear in saddle-node bifurcations, increases as they approach heteroclinicity. Such behaviour has been investigated in several related problems (Bernoff 1986; Weiss 1987; Swinton & Elgin 1990).

The existence of a chaotic attractor for the canonical system (15) and for the Lorenz system (14) with $\varpi \ll 1$ demonstrates that chaos does indeed occur in point-symmetric thermosolutal convection and that it is caused by the Shil'nikov mechanism. Chaotic behaviour has also been found numerically both for (14) and for the fifth-order model with ϖ of order unity but in regimes where they are no longer valid approximations to the partial differential equations. The latter have been

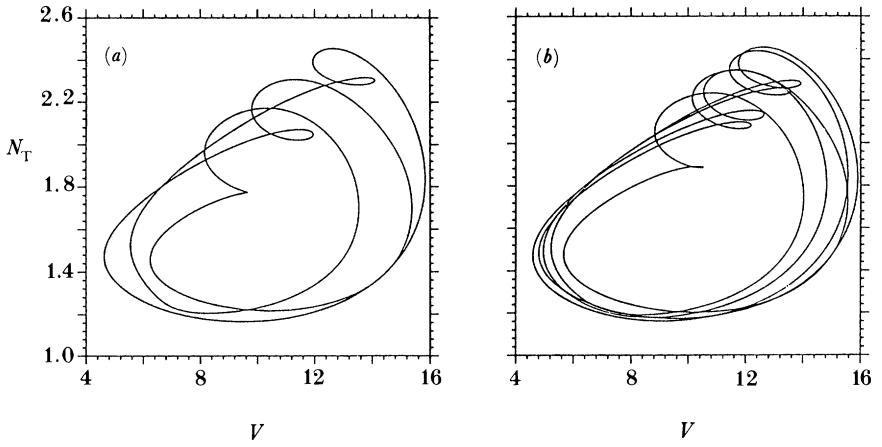

Figure 6. Periodic windows within the chaotic regime for the partial differential equations with $R_S = 10^4$ and $\lambda = 1.4$. Orbits projected onto the (V, N_T)-plane for (*a*) an S3 solution at $R_T = 10640$ and (*b*) an S5 solution at $R_T = 10609$. (After Moore *et al.* 1990*b*.)

solved numerically and chaotic behaviour consistent with the Shil'nikov mechanism can be recognized, e.g. for $\lambda = 1.5$ (Huppert & Moore 1976; Moore *et al.* 1983; Knobloch *et al.* 1986*b*; some phase portraits are reproduced by Weiss 1987, 1990*a*). When chaos appears in numerical experiments it is not always certain whether it is a property of the partial differential equations or a spurious consequence of discretization. It has indeed been suggested that chaos in computational studies of thermosolutal convection is an artefact caused by inadequate numerical resolution (Shi & Orszag 1987; Goldhirsch, Pelz & Orszag 1989). Moore *et al.* (1990*b*) conducted a careful study of the effects of discretization on the bifurcations; they found that while codimension-one bifurcation sets were simply displaced in parameter space, bifurcations of codimension two were more sensitive to numerical errors. It is not always practicable to keep refining the mesh and continuing the runs for longer times to see whether apparently chaotic behaviour persists. A better procedure is to locate periodic orbits and to follow them as the mesh is progressively refined. The presence of chaos was confirmed by tracking narrow S5 and S3 windows within the chaotic régime. Figure 6*a* shows an S3 orbit projected onto the (V, N_T)-plane, where the r.m.s. velocity V is given by

$$V^2 = (2\lambda)^{-1} \int_0^1 \int_0^\lambda |\nabla \psi^2| \, \mathrm{d}x \, \mathrm{d}z. \tag{17}$$

The corresponding S5 orbit is illustrated in figure 6*b*. The symmetry $t_x = it_z$ implies that each orbit in this plane is described twice in one period of the oscillation; within each window there is a sequence of bifurcations corresponding to behaviour in the map (16). The windows occur over a very narrow range in R_T: for instance, the position of the S5 window is determined to an accuracy of 1 in 10^4 and converges at a rate consistent with the accuracy of the difference scheme as the number of mesh intervals is increased from 40 to 160. Since the values of R_T for the S5 and S3 windows converge to different values the existence of all the associated bifurcation structure, including chaos, can be demonstrated conclusively.

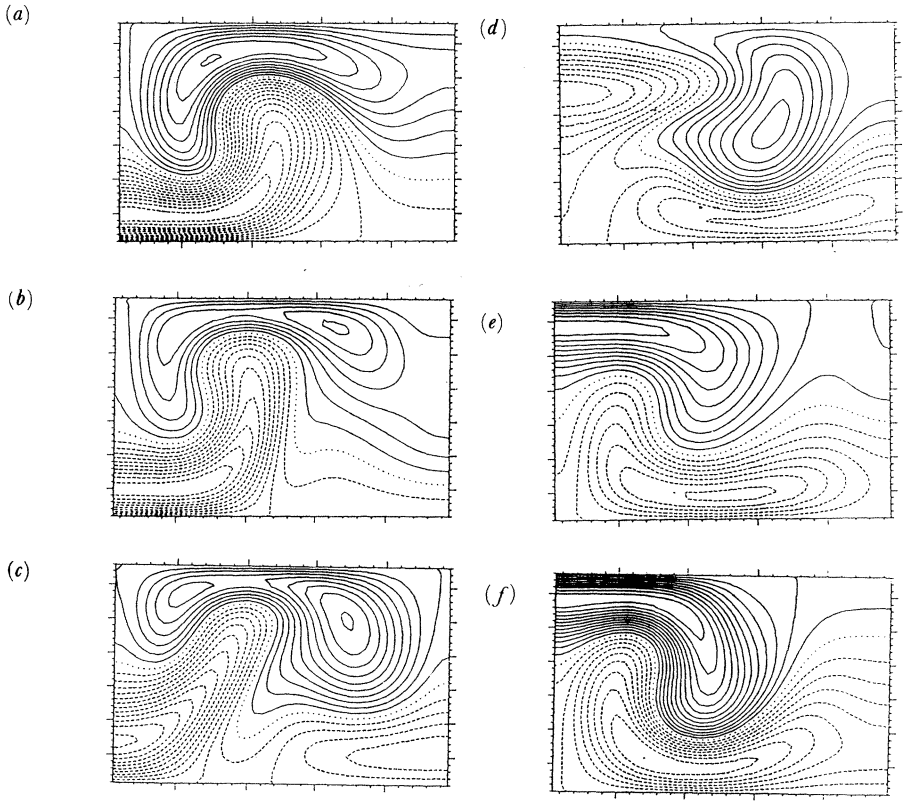

Figure 7. Loss of point symmetry. Contours of the normalized density ρ for a spatially asymmetric S1 oscillation with period $P = 0.4$ at times (*a*) $t = 0$, (*b*) $t = 0.04$, (*c*) $t = 0.08$, (*d*) $t = 0.12$, (*e*) $t = 0.16$, (*f*) $t = 0.20$. (After Moore *et al.* 1991.)

4. Loss of spatial symmetry

So far we have only considered bifurcations involving loss of temporal symmetries. Now we relax the imposed point symmetry (12), thereby allowing the symmetry i of the ss and sw solutions to be broken at secondary bifurcations. For $\lambda = 1.5$ solutions with point symmetry on the upper portion of the steady branch, like that exhibited in figure 1, are always stable with respect to asymmetric perturbations. We find, however, that oscillatory solutions lose point symmetry around $R_T = 10800$ and stable periodic solutions that are spatially symmetric can be found for $10690 \leqslant R_T \leqslant 11795$ (Moore *et al.* 1991). Figure 7 shows the normalized density

$$\rho(x, z, t) = R_S S - R_T T \tag{18}$$

for an S1 solution at $R_T = 10800$ at equally spaced intervals in time spanning approximately half a period. It is apparent that the point symmetry of figure 1 has been broken: action is concentrated on the left-hand side while the right-hand side is relatively static. (There is an equivalent solution, related by the broken symmetry to that in figure 7, with the action on the right.) Although both S and T vary smoothly the density shows much more structure, with isolated plumes and islands. Comparison of figure 7*a* with figure 7*f* shows that the symmetry t_z is still preserved.

The eigenfunctions of the linear problem have the form

$$\psi = \psi_{mn}(t) \sin(m\pi x/\lambda) \sin(n\pi z), \text{ etc.} \tag{19}$$

For $\lambda = 1.5$ the first Hopf bifurcation occurs at $R_T = 7725$ for $(m, n) = (1, 1)$, closely followed by a second Hopf bifurcation at $R_T = 8616$ for $(m, n) = (2, 1)$. The branch emerging from this second bifurcation corresponds to two-roll solutions which possess the symmetry

$$m_x: \quad (x, z) \to (\lambda - x, z), \quad (\psi, \theta, \Sigma) \to (-\psi, \theta, \Sigma) \tag{20}$$

but lack the symmetry i. Spatially asymmetric oscillations like that in figure 7 correspond to mixed-mode solutions on branches linking the branches of pure single-roll and two-roll solutions. It can readily be seen that a simple combination yields a horizontal structure of the form

$$\sin(\pi x/\lambda) + \epsilon \sin(2\pi x/\lambda) = \sin(\pi x/\lambda)[1 + 2\epsilon \cos(\pi x/\lambda)], \tag{21}$$

which reduces the amplitude of motion on the right or left of the region depending on the sign of ϵ, as found in figure 7. The full bifurcation structure, involving many branches, has been investigated for the analogous problem in magnetoconvection (Nagata *et al.* 1990).

If the aspect ratio is doubled so that $\lambda = 3$ trajectories are no longer attracted to solutions like that in figure 7. The first mode to become unstable has $m = 2$: this corresponds to the single-roll sw solution with $\lambda = 1.5$ but now it is followed successively by modes with $m = 3, 4$ and 1. Secondary, tertiary and subsequent bifurcations can rapidly lead to an intricate pattern of mixed modes. Figure 8 shows apparently persistent chaotic behaviour found for $R_T = 11\,100$ after the system has evolved from an initially perturbed state up to $t = 64$ (Moore *et al.* 1990*a*). The density contours plotted at six equally spaced points in time show strong rising and sinking plumes, with a tendency for disturbances to travel to the left. This example of spatiotemporal chaos shows that irregular behaviour is likely to develop unless the system is severely constrained by imposed symmetries or boundary conditions. Although motion is still dominated by coherent structures there is no obvious periodicity in space or time. In boxes with much larger aspect ratios aperiodic travelling waves progress from side to side and are reflected at the lateral boundaries (Deane *et al.* 1988).

5. Conclusion

Two-dimensional thermosolutal convection provides an idealized but instructive model that illustrates the range of behaviour possible in a nonlinear fluid system. In the configuration that we have studied here complicated behaviour occurs in the parameter range $0.91 \leqslant R_T/R_S \leqslant 1.19$ where double-diffusive effects lead to variations of density that produce dynamically interesting oscillations. With different boundary conditions or in three dimensions further instabilities would lead eventually to turbulent motion as in ordinary Bénard convection (Libchaber 1987; Castaing *et al.* 1989).

From a more mathematical point of view, we have shown how multiple bifurcations can lead to complicated spatiotemporal behaviour. This can be investigated in the laboratory or in numerical experiments where successive transitions can be isolated. Analysis of the bifurcation structure relies, however, on constructing low-order

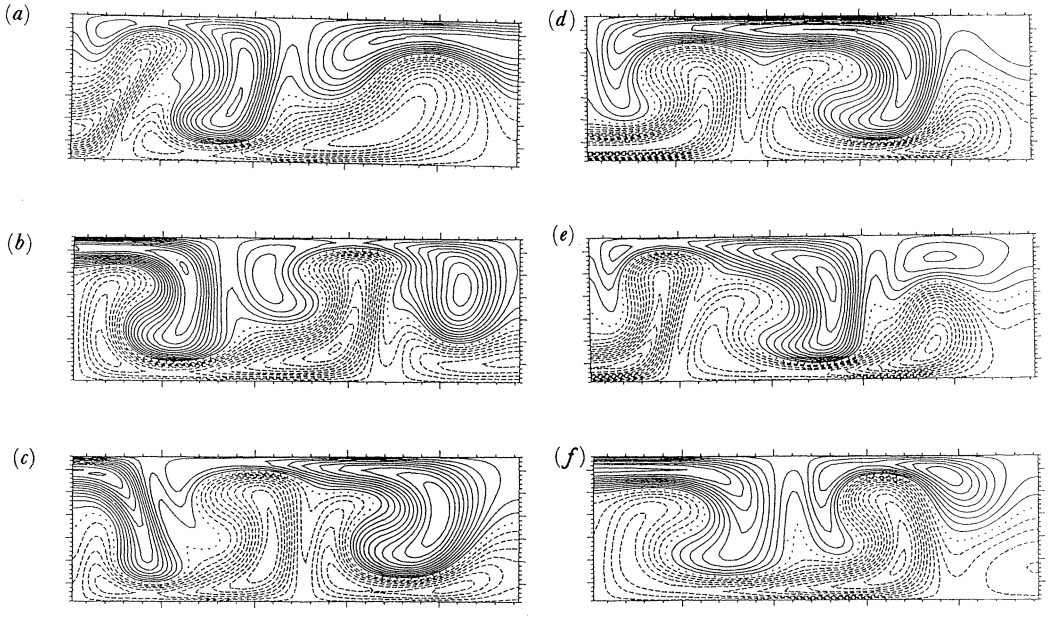

Figure 8. Spatiotemporal chaos in a domain with $\lambda = 3$. Contours of ρ at times (*a*) $t = 0.0$, (*b*) $t = 0.1$, (*c*) $t = 0.2$, (*d*) $t = 0.3$, (*e*) $t = 0.4$ and (*f*) $t = 0.5$, referred to an arbitrary origin.

evolution equations to describe the pattern that has been observed. This can be achieved by unfolding degenerate bifurcations to produce canonical normal form equations. The second-order Bogdanov–Takens equation (13) is an obvious example of this approach: the interaction between standing wave and steady solutions with Z_2 symmetry can be understood by reference to equation (13) and the normal form equations have been extended to cover travelling waves with $O(2)$ symmetry as well (Dangelmayr & Knobloch 1987). Temporal chaos requires a third-order system: the Lorenz equations (14) can be regarded as a simplified normal form for the degenerate bifurcation of codimension three that occurs when $\mu = \nu = \varpi = 0$ (Spiegel 1987). Loss of spatial symmetry with the formation of mixed-mode solutions can be treated similarly. The normal form equations for a double pitchfork or Hopf bifurcation are just a Lotka–Volterra system (Stuart 1962; Guckenheimer & Holmes 1986) and the interaction between sw and ss branches could be brought in by constructing a fourth-order coupled Bogdanov–Takens system (Weiss 1990*b*).

The same sort of approach can of course be applied to other problems. Magnetoconvection displays similar behaviour (Proctor & Weiss 1982) though the nonlinear Lorentz force allows a wider range of possibilities, especially if the fluid is compressible (Hughes & Proctor 1988; Hurlburt *et al.* 1989). Rotation also leads to an analogous bifurcation structure (Guckenheimer & Knobloch 1983; Silber & Knobloch 1989). The existence of chaos arbitrarily close to the onset of instability was first demonstrated for thermosolutal convection in a rotating system where the normal form equation is obtained by unfolding a degenerate bifurcation of codimension three with a triple-zero eigenvalue (Arnéodo *et al.* 1985; Arnéodo & Thual 1985). The resulting system is fundamentally different from (14) and (15) but closely related to the equation put forward long ago by Moore & Spiegel (1966; Spiegel 1985) to describe double convection, which yielded aperiodic oscillations.

What is remarkable is that the appearance of chaos in all these problems is associated with homoclinic or heteroclinic bifurcations involving a saddle-focus. The Shil'nikov mechanism crops up everywhere.

We have benefited from lively discussions with Edgar Knobloch and Michael Proctor and we are grateful to Janet Wilkins for assisting with the computation.

References

Ahlers, G. & Rehberg, I. 1986 *Phys. Rev. Lett.* **56**, 1373–1376.

Arnéodo, A., Coullet, P. H. & Spiegel, E. A. 1985 *Geophys. Astrophys. Fluid Dyn.* **31**, 11–48.

Arnéodo, A. & Thual, O. 1985 *Phys. Lett.* A **109**, 367–373.

Arnol'd, V. I. 1983 *Geometrical methods in the theory of ordinary differential equations*. Berlin: Springer.

Barten, W., Lücke, M., Hort, W. & Kamps, M. 1989 *Phys. Rev. Lett.* **63**, 376–379.

Bernoff, A. J. 1986 Transitions from order in convection. Ph.D. thesis, University of Cambridge, U.K.

Bretherton, C. S. & Spiegel, E. A. 1983 *Phys. Lett.* A **96**, 152–156.

Castaing, B., Gunaratne, G., Heslit, F., Kadanoff, L., Libchaber, A., Thomae, S., Wu, X., Zaleski, S. & Zanetti, G. 1989 *J. Fluid Mech.* **204**, 1–30.

Coullet, P. H. & Spiegel, E. A. 1983 *SIAM J. appl. Math.* **43**, 776–821.

Da Costa, L. N., Knobloch, E. & Weiss, N. O. 1981 *J. Fluid Mech.* **109**, 25–43.

Dangelmayr, G. & Knobloch, E. 1987 *Phil. Trans. R. Soc. Lond.* A **322**, 243–279.

Deane, A. E., Knobloch, E. & Toomre, J. 1987 *Phys. Rev.* A **36**, 2862–2869.

Deane, A. E., Knobloch, E. & Toomre, J. 1988 *Phys. Rev.* A **37**, 1817–1820.

Gaspard, P., Kapral, R. & Nicolis, G. 1984 *J. statist. Phys.* **35**, 697–727.

Glendinning, P. A. & Sparrow, C. T. 1984 *J. statist. Phys.* **35**, 645–696.

Goldhirsch, I., Pelz, R. B. & Orszag, S. A. 1989 *J. Fluid Mech.* **199**, 1–28.

Guckenheimer, J. & Holmes, P. 1986 *Nonlinear oscillations, dynamical systems and bifurcations of vector fields*. New York: Springer.

Guckenheimer, J. & Knobloch, E. 1983 *Geophys. Astrophys. Fluid Dyn.* **23**, 247–272.

Hughes, D. W. & Proctor, M. R. E. 1988 *A. Rev. Fluid Mech.* **20**, 187–223.

Huppert, H. E. & Moore, D. R. 1976 *J. Fluid Mech.* **78**, 821–854.

Huppert, H. E. & Turner, J. S. 1981 *J. Fluid Mech.* **106**, 299–329.

Hurlburt, N. E., Proctor, M. R. E., Weiss, N. O. & Brownjohn, D. P. 1989 *J. Fluid Mech.* **207**, 587–628.

Knobloch, E., Deane, A. E., Toomre, J. & Moore, D. R. 1986*a* *Contemp. Maths.* **56**, 203–216.

Knobloch, E. & Moore, D. R. 1990 *Phys. Rev.* A. (In the press.)

Knobloch, E., Moore, D. R., Toomre, J. & Weiss, N. O. 1986*b* *J. Fluid Mech.* **166**, 409–448.

Knobloch, E. & Proctor, M. R. E. 1981 *J. Fluid Mech.* **108**, 291–316.

Knobloch, E., Proctor, M. R. E. & Weiss, N. O. 1990 *J. Fluid Mech.* (Submitted.)

Knobloch, E. & Silber, M. 1990 *Geophys. Astrophys. Fluid Dyn.* **51**, 195–209.

Libchaber, A. 1987 *Proc. R. Soc. Lond.* A **413**, 63–69.

May, R. M. 1976 *Nature, Lond.* **261**, 459–467.

Metropolis, N., Stein, M. L. & Stein, P. R. 1973 *J. Comb. Theor.* A **15**, 25–44.

Moore, D. R. & Knobloch, E. 1990 *Phys. Rev. Lett.* (Submitted.)

Moore, D. R., Toomre, J., Knobloch, E. & Weiss, N. O. 1983 *Nature, Lond.* **303**, 663–667.

Moore, D. R., Weiss, N. O. & Wilkins, J. M. 1990*a* *Phys. Lett.* A. (In the press.)

Moore, D. R., Weiss, N. O. & Wilkins, J. M. 1990*b* *Nonlinearity*. (In the press.)

Moore, D. R., Weiss, N. O. & Wilkins, J. M. 1991 *J. Fluid Mech.* (Submitted.)

Moore, D. R. & Spiegel, E. A. 1966 *Astrophys. J.* **143**, 871–887.

PHILOSOPHICAL TRANSACTIONS OF THE ROYAL SOCIETY A MATHEMATICAL, PHYSICAL & ENGINEERING SCIENCES

Nagata, M., Proctor, M. R. E. & Weiss, N. O. 1990 *Geophys. Astrophys. Fluid Dyn.* **51**, 211–241.

Padman, L. & Dillon, T. M. 1987 *J. geophys. Res.* **92**, 10799–10806.

Proctor, M. R. E. & Weiss, N. O. 1982 *Rep. Prog. Phys.* **45**, 1317–1379.

Proctor, M. R. E. & Weiss, N. O. 1990 *Nonlinearity*. (In the press.)

Ruelle, D. 1973 *Arch. ration. Mech. Analysis* **51**, 136–152.

Shi, A. & Orszag, S. A. 1987 Preprint.

Shil'nikov, L. P. 1965 *Soviet Math. Dokl.* **6**, 163–166.

Sparrow, C. T. 1982 *The Lorenz equations: bifurcations, chaos and strange attractors*. New York: Springer.

Spiegel, E. A. 1985 In *Chaos in astrophysics* (ed. R. Buchler, J. Perdang & E. A. Spiegel), pp. 91–135. Dordrecht: Reidel.

Spiegel, E. A. 1987 *Proc. R. Soc. Lond.* A **413**, 87–95.

Stewart, I. N. 1988 In *New directions in dynamical systems* (ed. T. Bedford & J. W. Swift), pp. 233–283. Cambridge University Press.

Stuart, J. T. 1962 In *Applied mechanics* (ed. F. Rolla & W. T. Koiter), pp. 63–97. Amsterdam: Elsevier.

Swinton, J. & Elgin, J. N. 1990 *Phys. Lett.* A. (Submitted.)

Veronis, G. 1965 *J. mar. Res.* **23**, 1–17.

Veronis, G. 1968 *J. Fluid Mech.* **34**, 315–336.

Walden, R. W., Kolodner, P., Passner, A. & Surko, C. M. 1985 *Phys. Rev. Lett.* **55**, 496–499.

Weiss, N. O. 1987 *Proc. R. Soc. Lond.* A **413**, 71–85.

Weiss, N. O. 1990*a* *Phil. Trans. R. Soc. Lond.* A **330**, 617–625.

Weiss, N. O. 1990*b* In *Nonlinear evolution of spatio-temporal structures in dissipative continuous systems* (ed. F. Busse & L. Kramers). New York: Plenum Press.

Wiggins, S. 1988 *Global bifurcations and chaos*. New York: Springer.

PHILOSOPHICAL TRANSACTIONS OF THE ROYAL SOCIETY A MATHEMATICAL, PHYSICAL & ENGINEERING SCIENCES